Journal of
Ceramic Science
and Technology

J. Ceram. Sci. Tech., **03** [02] 61-68 (2012)
DOI: 10.4416/JCST2012-00005
available online at: http://www.ceramic-science.com

Laser Synthesis of Al_2TiO_5 Ceramics from Al_2O_3-TiO_2 Powder Mixtures

M. Vlasova*[1], B. Sosa Coeto[1], M. Kakazey[1], P. A. Marquez Aguilar[1], I. Rosales[1], A. Escobar Martinez[1], V. Stetsenko[2], A. Bykov[2]

[1]Center of Investigation in Engineering and Applied Sciences of the Autonomous University of the State of Morelos (CIICAp-UAEMor), Av. Universidad, 1001, Cuernavaca, Mexico.
[2]Institute for Problems of Materials Science, National Academy of Sciences of Ukraine, 3, Krzhyzhanovsky St., Kiev, 252680, Ukraine

received January 25, 2012; received in revised form February 26, 2012; accepted March 21, 2012

Abstract

The phase formation process in the zone of laser irradiation of Al_2O_3-TiO_2 compacts with different contents of components has been investigated with XRD, electron microscopy, and atomic force microscopy methods. The distinctive feature of laser synthesis is the simultaneous formation of α-and β-Al_2TiO_5, which is caused by the non-uniform heating of the material in the irradiation zone. The motion of the eutectic melt under the action of hydrodynamic forces is the motive force for texturing of precipitating crystalline phases during fast cooling. The degree of texturing of Al_2O_3 and Al_2TiO_5 crystallites depends on the amount of the formed eutectic melt.

Keywords: Al_2O_3, TiO_2, laser treatment, Al_2TiO_5

I. Introduction

Owing to its superior thermal properties such as low thermal expansion and thermal conduction coefficients, high melting point, high corrosion resistance, and thermal shock resistance, aluminium titanate ceramic is classified with high-temperature materials used under conditions of large thermal loads [1–6].

Different methods of preparing aluminium titanate powders [7–10] and aluminium-titanate-based ceramics are known. These include various variants of solid-phase sintering of titanium and aluminium oxides, melt synthesis, spark plasma sintering, etc. [7,11–15]. To improve the thermomechanical stability of Al_2TiO_5 ceramics, laser surface treatment, which is based on directional solidification of eutectics, is used [16–17].

Recent investigations have shown that effects of rapid remelting of the surface layer of the ceramic followed by fast cooling and rapid crystallization substantially change the texture of the surface [16–19]. At present, macro-, micro-, and nanotexturing are distinguished. The character of texturing depends on the power of radiation, traversing speed of the laser beam, and the composite composition of the material. Since high temperatures are achieved in the irradiation zone [20], it can be assumed that the synthesis-sintering-texturing effects may be combined into one process. The synthesized material must have a phase state differing to some degree from that obtained in common solid-phase sintering and it must be surface- and volume-textured.

* Corresponding author:
vlasovamarina@unbox.ru;kakazey@hotmail.com

The aim of the present work is to investigate phase formation and texturing in the irradiation zone of compacted Al_2O_3-TiO_2 powder mixtures with different contents of the components.

II. Experimental Procedure

In the present work, specimens were prepared from analytically pure Al_2O_3 and TiO_2 powders (produced by REASOL).

Type 1 Specimens. An aluminium oxide powder and a 54 mol% Al_2O_3-46 mol% TiO_2 powder mixture were compacted in pellets with a diameter of 18 mm and a thickness of 2 – 3 mm under a pressure of 7 MPa.

As a result of irradiation, concave channels (tracks) formed on the surfaces of specimens. These tracks were easily removed from the compacts. The lower sides of the tracks were cleaned to remove the loose slightly sintered powder.

Type 2 Specimens. A series of cylindrical pellets with a diameter of 5 mm and a length of 7 mm were isostatically pressed from Al_2O_3-x TiO_2 powder mixtures, where x = 0.127, 0.54, 1.27, 6.29 and 12.41 mol% at a pressure of 5 GPa. On the surfaces of pellets annular tracks, firmly bonded to the compacts, were formed.

Laser treatment was performed in an LTN-103 unit (continuous-action laser with $\lambda = 1064$ nm). In irradiation of **Type 1** specimens, the power of radiation (P) was 120 W, the diameter of the beam (d) was 1.5 mm, and the linear traversing speed of the beam was $v = 0.15$ mm/s. The angle of incidence of the laser beam on the sample surface was 45°. A simplified scheme of the irradiation is shown in

Fig. 1. **Type 2** specimens were irradiated at $P = 130$ W and $d = 1.5$ mm by traversing the laser beam around a circle at $v = 0.7$ mm/s. The laser beam was at an angle of 45° to the surface.

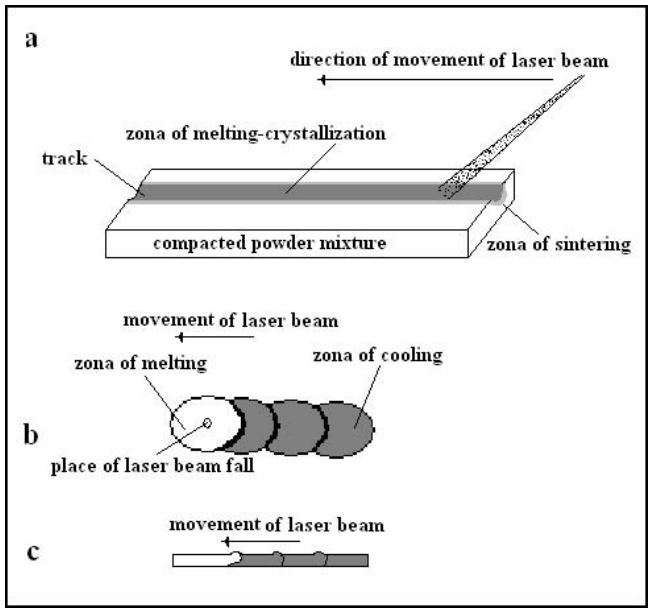

Fig. 1 : A simplified scheme showing the irradiation of the mixtures (a); overlay zones of heating and cooling with a moving laser beam (b, c); a top view of track (b); a side view of track (c).

The synthesis products were investigated with the X-ray diffraction (XRD) method in Cu K_α radiation (a DRON-3M diffractometer, Russia). An electron microscopy study and an electron-probe microanalysis were performed with a HU-200F type scanning electron microscope and a LEO 1450 VP unit. An atomic force microscopy investigation (Digital Instruments Nanoscope IV in tapping mode with a silicon nitride tip) was conducted in amplitude regimes.

III. Results

(1) Type 1 Specimens

In the zone of laser irradiation of Al_2O_3 compacts and compacts obtained from the 54 mol% Al_2O_3-46 mol% TiO_2 powder mixture, channels form (Fig. 2a, b). Their formation is associated with high temperatures in the irradiation zone, owing to which the sintering and melting-solidification processes proceed simultaneously [20].

According to XRD analysis data, in irradiated aluminium oxide compacts, the channel material is α-Al_2O_3 (Figs. 3a, b). The channel material of the specimens compacted from the 54 mol% Al_2O_3-46 mol% TiO_2 contained, basically, the β-Al_2TiO_5 and α-Al_2TiO_5 crystalline phases, a small amount of Al_2O_3, and traces of TiO_2 (Fig. 3c). An analysis of the intensities of diffraction lines of Al_2TiO_5 and Al_2O_3 revealed the distortion of the ratio of intensities (Table 1), which is characteristic of textured materials.

Table 1: The ratio of intensity of X-ray diffraction lines for the phases α-Al_2O_3 and β-Al_2TiO_5

Type of specimen	Phase	I_1/I_2	Standard	After irradiation
Al_2O_3	α-Al_2O_3	$I_{(104)}/I_{(116)}$	1.1	0.71
54 mol% Al_2O_3 - 46 mol% TiO_2	β-Al_2TiO_5 α-Al_2O_3	$I_{(230)}/I_{(531)}$ $I_{(104)}/I_{(116)}$	2.26 1.1	0.32 0.068

The electron-probe microanalysis showed the presence of only Al and O in the channel material of the Al_2O_3 compact (Fig. 4a) and the presence of Al, Ti, and O in the channel material of the irradiated mixture (Fig. 4b).

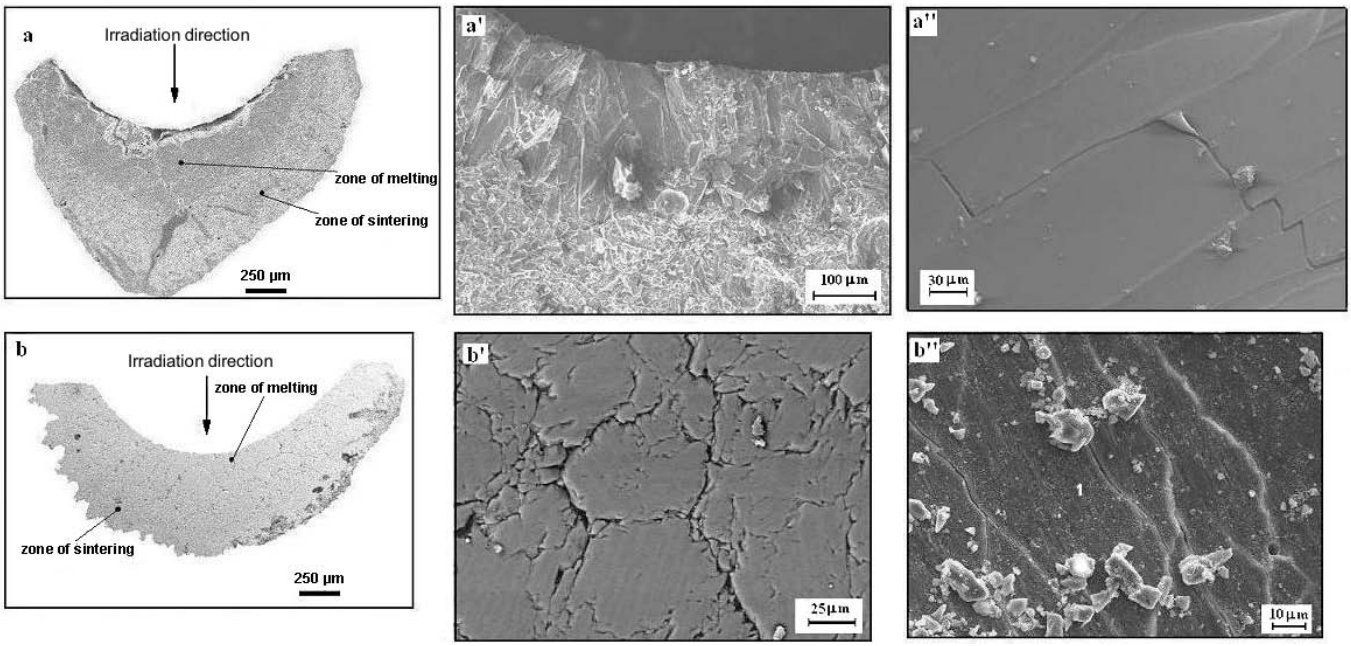

Fig. 2 : Electron micrographs of channels formed after laser irradiation of specimens compacted from Al_2O_3 powder (a, a', a'') and a 54 mol% Al_2O_3-46 mol% TiO_2 powder mixture. (b, b', b''). (a, a', b, b') cross-section of the channel; (a'', b'') top view.

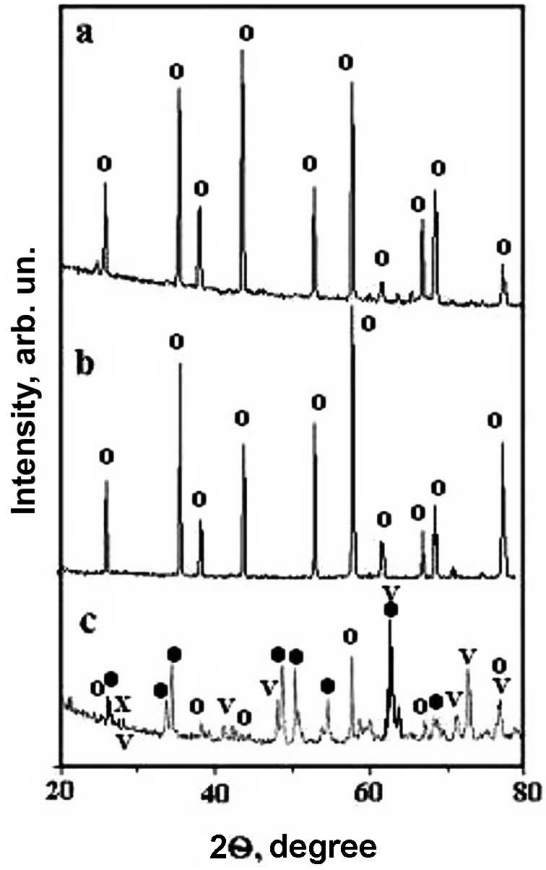

Fig. 3: Fragments of X-ray diffraction patterns of the initial Al_2O_3 powder(a), track material on the surface of an Al_2O_3 compact (b), track material on the surface of a 54 mol% Al_2O_3-46 mol% TiO_2 compact (c). (•) α-Al_2TiO_5; (v) β-Al_2TiO_5; (o) Al_2O_3; (x) TiO_2.

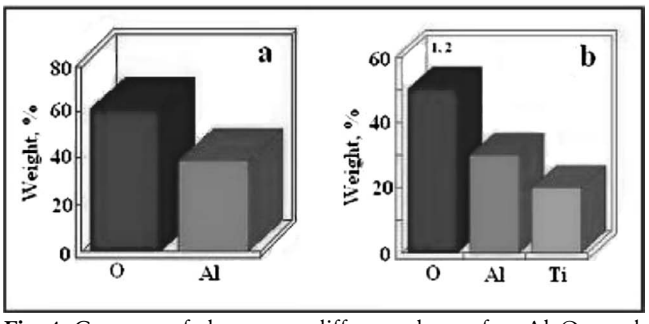

Fig. 4: Contents of elements at different places of an Al_2O_3 track (a) and an Al_2TiO_5 track (b). 1 and 2 correspond to places 1 and 2, respectively, in Fig. 1b''.

The surfaces of channels are represented by, respectively, Al_2O_3 and Al_2TiO_5 grains, textured along the direction of traversing of the laser beam (Figs. 2a'', b''). On Al_2TiO_5 grains, we can see longitudinal traces in the form of tracks, which are characteristic of lamellae formation (Fig. 2b''). Microcracks and pores are located along grain boundaries and between them. On a cross-section of a channel (Figs. 2a, b), it can be seen that the body of the channel consists of different zones. The upper part of the channel is the zone of melting and recrystallization of Al_2O_3 and Al_2TiO_5 grains, the sizes of which increase as the distance to the surface of the channel decreases (Fig. 2a', b). The lower part of the channel is the sintering zone. The AFM data indicate that Al_2TiO_5 grains consist of nanoparticles with a size of ~7 nm, which form chains of different length and orientation.

(2) Type 2 Specimens

As noted above, after laser treatment of Al_2O_3-x TiO_2 dense compacts (where $x \leq 12.41$ mol%), convex torus-like tracks with a hollow at the centre form on their surfaces (Fig. 5a). The causes of formation of the tracks are high temperatures achieved in the irradiation zone of dense compacts and the fairly large width of the laser beam with regard to its defocusing relative to the diameter of the compact. As a result, longer heating at the centre and the transfer of the melt of the material to the periphery take place (see Fig. 5b).

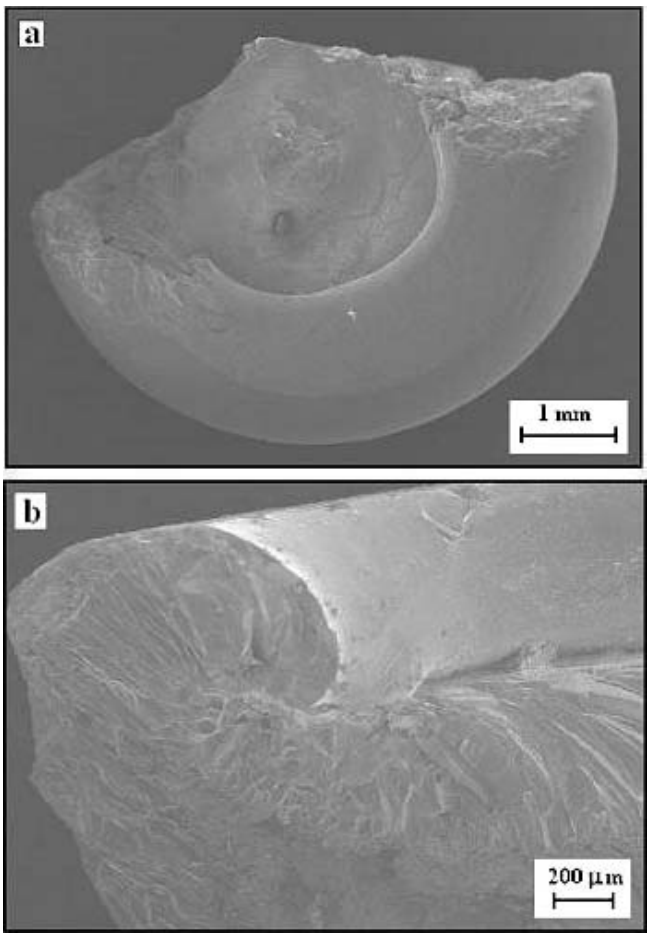

Fig. 5: Image of a track on the surface of a 99.873 mol% Al_2O_3-0.127 mol% TiO_2 dense compact after irradiation.

According to the XRD analysis data, α-Al_2O_3 is the major crystalline phase of the torus material (Fig. 6). Only in specimens prepared from mixtures with TiO_5 contents $c \geq 6.29$ mol% was the α-Al_2TiO_5 phase identified (Fig. 6d). An analysis of the intensities of Al_2TiO_5 diffraction lines revealed the distortion of the ratio of intensities (Figs. 6, 7), which indicates the texturing of the track material. The character of texturing is different for specimens of different composition and correlates with the TiO_2 content in the initial mixtures and the amount of formed Al_2TiO_5 in the tracks.

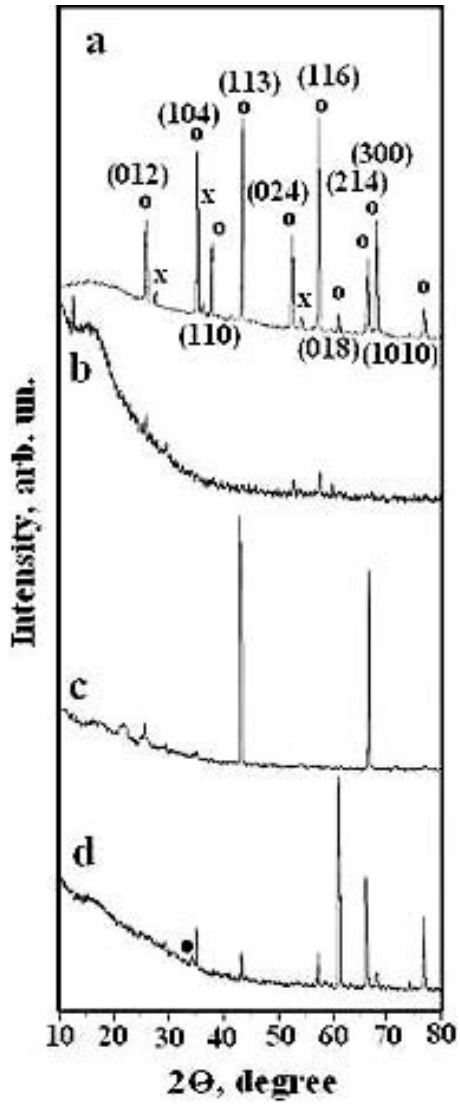

Fig. 6: Fragments of X-ray diffraction patterns of the initial powder mixture 93.71 mol% Al_2O_3-6.29 mol% TiO_2 (a) and track materials obtained as a result of laser irradiation of a 99.873 mol% Al_2O_3-0.127 mol% TiO_2 (b); a 98.73 mol% Al_2O_3-1.27 mol% TiO_2 (c), and a 93.71 mol% Al_2O_3-6.29 mol% TiO_2 compact (d). (o) Al_2O_3; (x) TiO_2; (•) Al_2TiO_5.

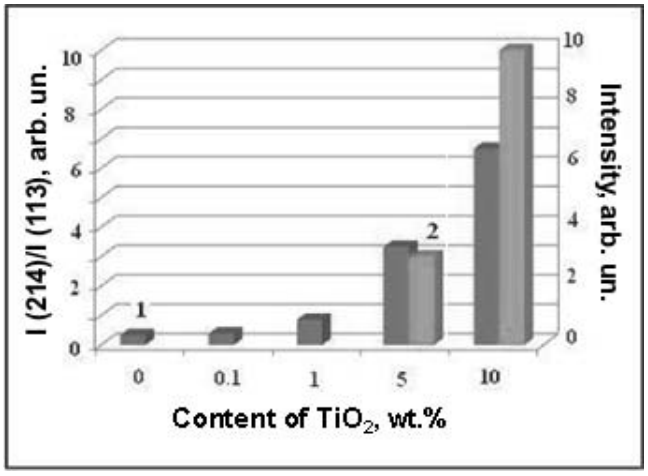

Fig. 7: Change in the ratio of the intensities of the (214) and (113) X-ray diffraction lines of Al_2O_3 and the intensity of the line α-Al_2TiO_5 in a torus depending on the TiO_2 content in the initial mixtures. (1) $I_{(214)}/I_{(113)}$; (2) $I_{\alpha\text{-}Al_2TiO_5}$ with d = 0.260 nm.

It can be seen in micrographs of specimens with a small TiO_2 content (from 0.127 mol% to 0.62 mol%) that the torus surface is smooth (Figs. 5b; 8 and 9a, b). With an increase in the TiO_2 content in the initial mixtures, on the surfaces of irradiated specimens (tori), roughness with indications of texturing emerges (see Figs. 8b – d). The direction of texturing coincides with the traversing direction of the laser beam and, as it follows from Figs. 9a, b, with motion of the liquid phase. On a fracture of the specimen (Fig. 9c), we also see texturing in the volume of the torus. As in the case of loose compacts, the coarsening of Al_2O_3 grains (crystallites) occurs in the direction towards the surface (see Fig. 2a').

IV. Discussion

In analysis of the experimental data, it is necessary to take into account the following features of laser treatment: at the used power of radiation, local temperatures on the surface of the specimen can attain 2000 °C [19]; the high-temperature heating of compacted specimens is realized in a narrow zone. As a result of traversing of the laser beam, the fast heating stage is followed by the fast cooling stage; depending on the thermal conductivity and the density of the material, diameter of the laser beam, and degree of its defocusing, in different regions of the material and at different depths of compacts, zones of different temperature form, i.e. a radial and a vertical temperature gradient exist [19, 21].

The studied Al_2O_3-TiO_2 powder compositions form liquid eutectics in temperature treatment. Depending on the ratio of the components and temperature in cooling of the melt, different phases crystallize [22, 23]. As can be seen from Fig. 3c, on irradiation of 54 mol% Al_2O_3-46 mol% TiO_2 compacts, α-and β-Al_2TiO_5 form simultaneously. Taking into account the presence of the temperature gradient, it can be assumed that this is caused by the simultaneous formation of different temperature zones in the compact. For instance, α-Al_2TiO_5 must form in the zone of higher temperature (the surface zone of the channel). The presence of Al_2O_3 and traces of TiO_2 indicate the partial decomposition of Al_2TiO_5 into Al_2O_3 and TiO_2 [24] and participation of ions Ti^{4+} in formation of α-phase [25]. The β-phase must form in zones of lower temperature that are adjacent to the sintering zone [24, 9].

The powder mixtures used for preparing **Type 2** specimens correspond to the alumina-rich region of the constitution diagram (see Fig. 10). Only with an increase in the TiO_2 content (see Fig. 6), conditions of formation of the eutectic melt and, as a result, conditions of crystallization of Al_2O_3 and Al_2TiO_5 in cooling are formed. Under the action of hydrodynamic forces [26–28], which arise in the longitudinal direction of the traversing of the laser beam, liquid executes directional motion. As a result, both Al_2O_3 crystallites and Al_2TiO_5 crystallites become textured during cooling (see Fig. 9). The degree of texturing increases as the content of the liquid phase increases (see Fig. 7). The major phase of **Type 2** specimens is Al_2O_3, and corundum crystallites form a crystalline skeleton. Aluminium titanate Al_2TiO_5 plays the role of the second phase, and its crystallites must be located between Al_2O_3 crystallites.

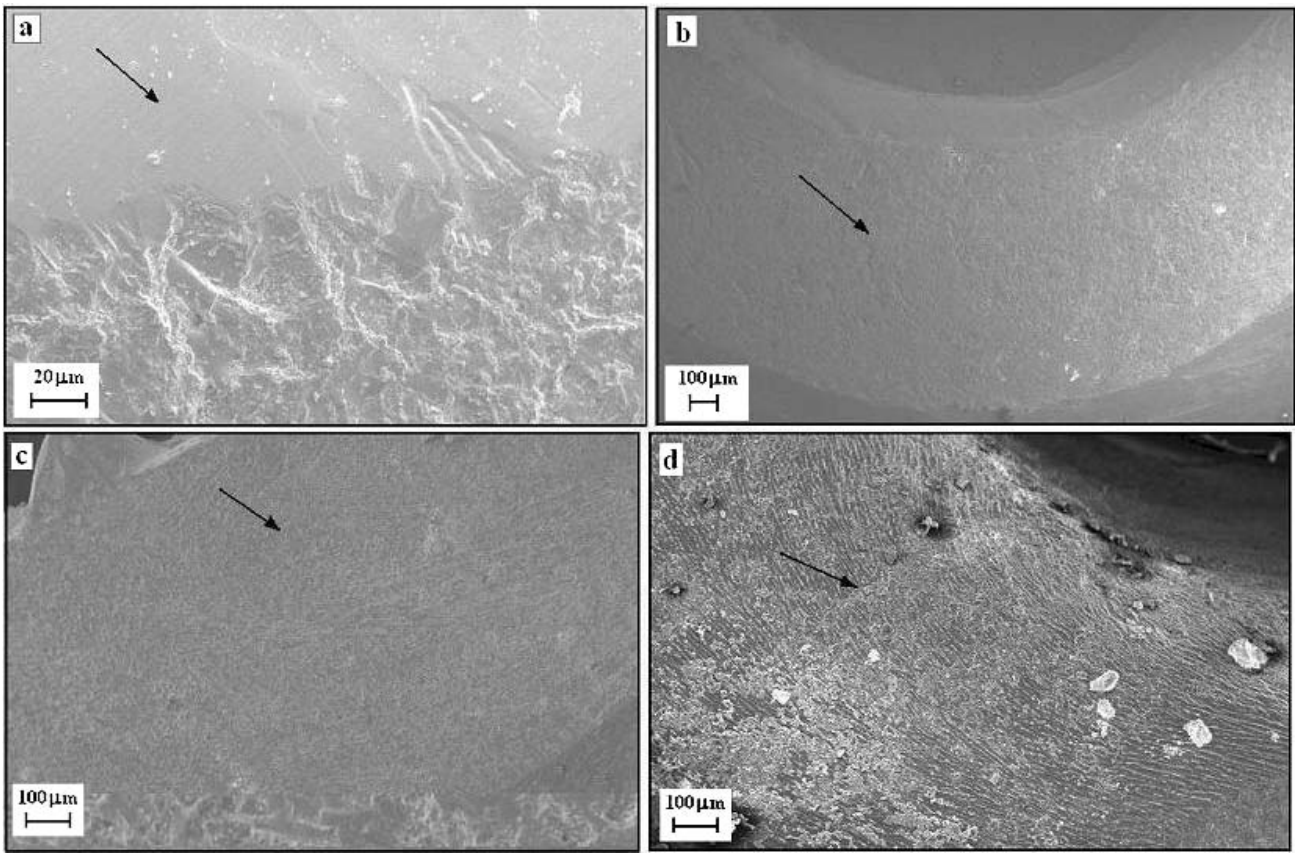

Fig. 8: Images of the surfaces of tracks formed as a result of irradiation of dense compacts obtained from a 99.36 mol% Al_2O_3-0.64 mol% TiO_2 (a), a 98.73 mol% Al_2O_3-1.27 mol% TiO_2 (b), a 93.71 mol% Al_2O_3-6.29 mol% TiO_2 (c), and a 87.59 mol% Al_2O_3-12.41 mol% TiO_2 (d) mixture. The surface is marked by an arrow.

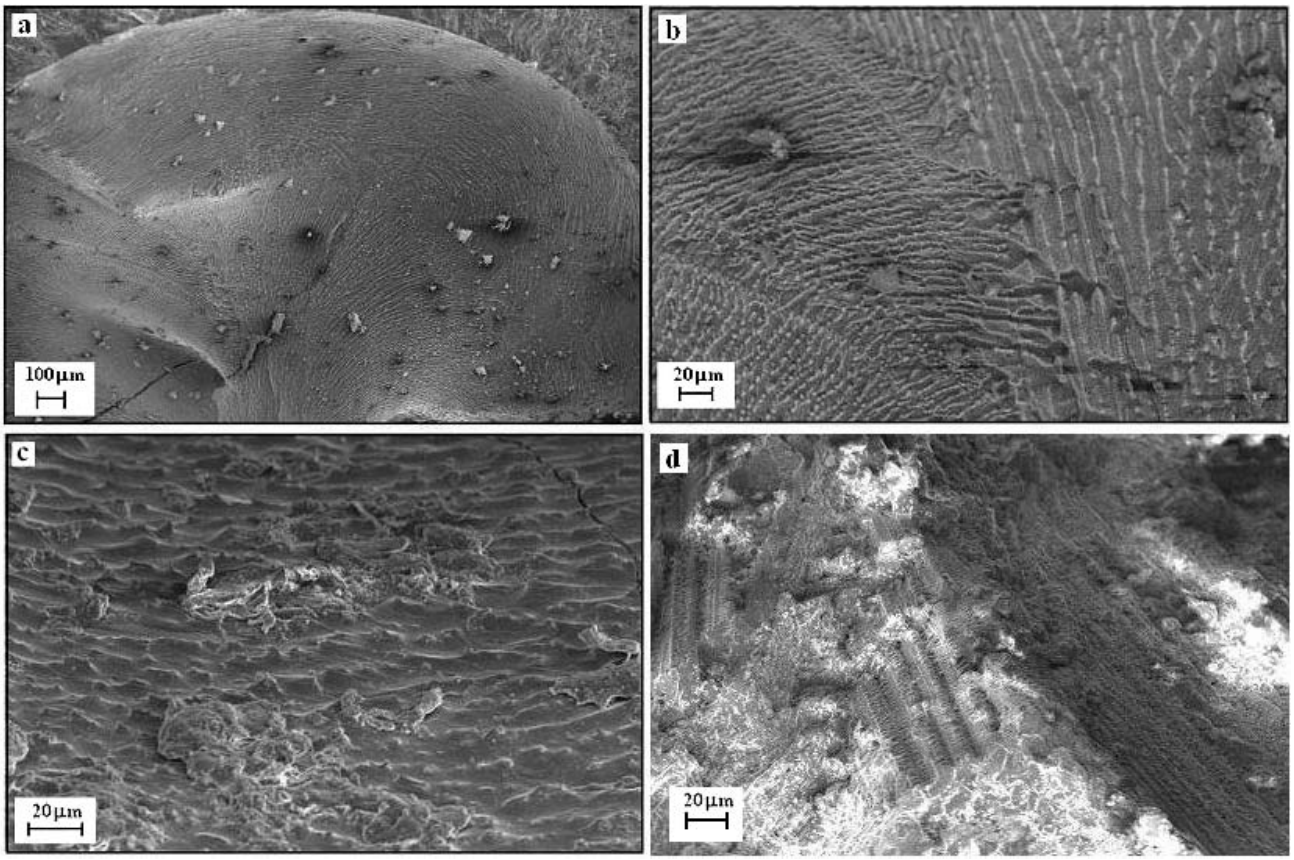

Fig. 9: Images of the surface of a track (a-c) formed on irradiation of a dense compact obtained from a 87.59 mol% Al_2O_3-12.41 mol% TiO_2 mixture. (d) fracture of the specimen.

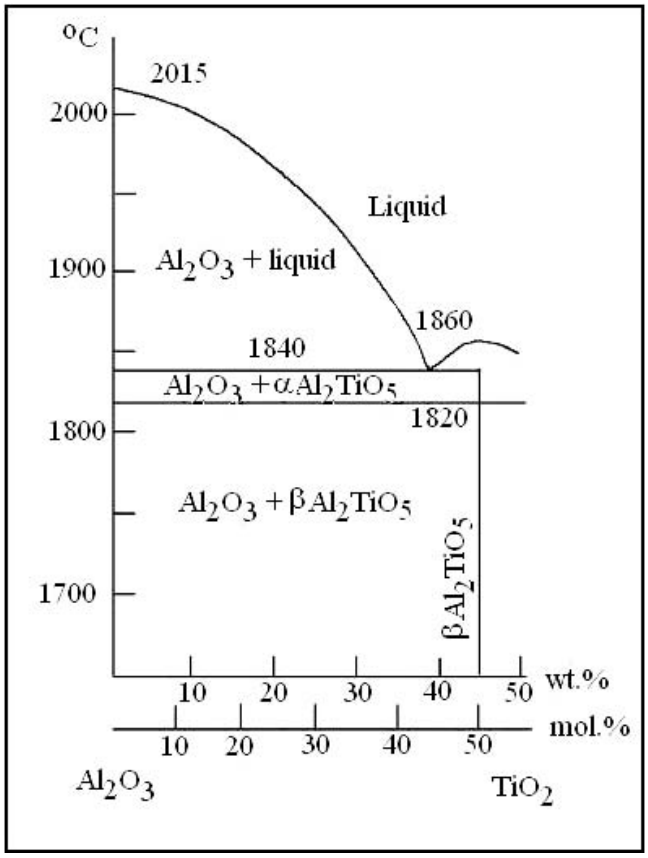

Fig. 10: Fragment of a constitution diagram of the Al_2O_3-TiO_2 system in the region of high corundum content [19].

Thus the investigations performed showed that as the laser beam traverses over the surface of compacted Al_2O_3-TiO_2 powder mixtures in the zone of fast heating, Al_2TiO_5 is synthesized in a certain volume of the material, and in the zone of fast cooling, texturing of the surface layer occurs.

V. Conclusions

The performed investigations showed the following:

- laser treatment of compacted Al_2O_3-TiO_2 powder mixtures with a high Al_2O_3 content is accompanied by the formation of the same crystalline phases as those present in the constitution diagram;
- the distinctive feature of the laser synthesis is the formation of α-and β-Al_2TiO_5, which is caused by the non-uniform heating of the material in the irradiation zone;
- the motion of the eutectic melt under the action of hydrodynamic forces is the motive force of texturing of precipitating crystalline phases during cooling;
- with increasing density of the compacts a texturing of the surface begins corresponding to texturing of the ceramic samples which were subjected to horizontally directed laser remelting.

References

1 Han, Ch., Selb, D.: Improving aluminium-titanate ceramics, (in German), *Sprechsaal*, **118**, [12], 1157 – 1166, (1985).

2 Ishitsuka, M., Sato, T., Endo, T., Shimada, M.: Synthesis and thermal stability of aluminium titanate solid solutions, *J. Am. Ceram. Soc.*, **70** [2], 69 – 71, (1987).

3 Thomas, H.A., Stevens, R.: Aluminium titanate – A literature review, part 1: Microcracking phenomena, *Br. Ceram. Trans. J.*, **88**, 144 – 151, (1989).

4 Kim, I.J., Kwak, H.S.: Thermal shock resistance and thermal expansion behaviour with composition and microstructure of Al_2TiO_5 ceramics, *Can. Metall. Quart.*, **39** [4], 387 – 395, (2000).

5 Sekar, M.M.A., Patil, K.C.: Synthesis and properties of tialite, β-Al_2TiO_5, *Brit. Cer. T.*, **93** [4], 146 – 9, (1994).

6 Oo, Z., Low, I.M.: Indentation responses of functionally-graded Al_2TiO_5-based ceramics, in: Advanced materials research, 239 – 242, 171 – 174, 2011. Eds. Zhong Cao, Xueqiang Cao, Lixian Sun, Yinghe He, DOI 10.4028/www.scientific.net/AMR.239 – 242.171.

7 Zaharescu, M., Crisan, M., Preda, M., Fruth, V., Preda, S.: Al_2TiO_5-based ceramics obtained by hydrothermal processes, *J. Optoelectron. Adv. M.*, **5**, [5], 1411 – 1416, (2003).

8 Neppolian, B., Wang, Q., Jung, H., Choi, H.: Ultrasonic-assisted sol-gel method of preparation of TiO_2 nano-particles: Characterization, properties and 4-chlorophenol removal application, *Ultrason. Sonochem.*, **15**, [4], 649 – 658, (2008).

9 Camaratta, R., Acchar, W., Bergmann, C.P.: Phase transformations in the Al_2O_3/TiO_2 system and metastable phase formation at low temperatures, *Rev. Adv. Mater. Sci.*, **27**, 64 – 68, (2011).

10 Stanciu, L., Groza, J.R., Stoica, L., Plapcianu, C.: Influence of powder precursors on reaction sintering of Al_2TiO_5, *Scripta Mater.*, **50**, 1259 – 1262, (2004).

11 Nagano, M., Nagashima, S., Maeda, H., Kato, A.: Sintering behavior of Al_2TiO_5 base ceramics and their thermal properties, *Ceram. Int.*, **25** [8], 681 – 687, (1999).

12 Norberg, S.T., Ishizawa, N., Hoffmann, S., Yoshimura, M.: Redetermination of β-Al_2TiO_5 obtained by melt casting, *Acta Crystallogr.*, Section E61, i160 – i162, (2005).

13 Huang, C.-L., Wang L.-J.: Microwave dielectric properties of sintered alumina using nano-scaled powders of a alumina and TiO_2, *J. Am. Ceram. Soc.*, **90** [5], 1487 – 1493, (2007).

14 Hoffmann, S., Norberg, S.T., Yoshimura, M.: Melt Synthesis of Al_2TiO_5 Containing composites and reinvestigation of the phase diagram Al_2O_3-TiO_2 by powder x-ray diffraction, *J. Electroceram.*, **16**, N. 4, 327 – 330, (2006).

15 Duan, R.-G., Zhan, G.-D., Kuntz, J. D., Kear, B.H., Mukherjee, A.K.: Spark plasma sintering (SPS) consolidated ceramic composites from plasma-sprayed metastable Al_2TiO_5 powder and Nano-Al_2O_3, TiO_2, and MgO powders, *Mater. Sci. Eng. A*, **373**, [1 – 2], 180 – 186, (2004).

16 LLorca, J., Orera, V.M.: Directionally solidified eutectic ceramic oxides, *Prog. Mater. Sci.*, **51**, 711 – 809, (2006).

17 Orera, V.M., Merino, R.I., Pardo, J.A., Larrea, A.A., Peña, J.I., Gonzalez, C., Poza, P., Pastor, J.Y., LLorca, J.: Microstructure and physical properties of some oxide eutectic composites processed by directional solidification, *Acta Mater.*, **48** [18/19], 4683 – 4689, (2000).

18 Su, H, Zhang, J., Deng, Y., Liu, L., Fu, H.: A modified preparation technique and characterization of directionally solidified $Al_2O_3/Y_3Al_5O_{12}$ eutectic *In Situ* composites, *Scripta Mater.*, **60**, [2], 362 – 365, (2009).

19 Berger, M.-H., Sayir, A.: Directional solidification of Al_2O_3-Al_2TiO_5 system, *J. Eur. Ceram. Soc.*, **28**, 2411 – 2419, (2008).

20 Vlasova, M., Kakazey, M., Márquez Aguilar, P.A.: Microstructural Evolution in α-Al_2O_3 Compacts during laser irradiation, Chapter in book: Advances in Ceramics. Synthesis and Characterization, Processing and Specific Application, Ed. Costas Sikalidis//Niksa Mandic . ISBN 978 – 953 – 307 – 505 – 1. INTECH - Open Access Publisher, 2011. pp. 393 – 420.

[21] Heinrich, J.G., Gahler, A., Günster, J., Schmücker, M., Zhang, J., Jiang, D., Ruan, M.: Microstructural evolution during direct laser sintering in the Al_2O_3-SiO_2 system, *J. Mater. Sci.*, **42**, 5307 – 5311, (2007).

[22] Toropov, N.A.: State Diagrams of Silicate Systems, 2nd ed., Leningrad, Nauka, 1969.

[23] Butting, E.N.: Phase equilibrium in the system TiO_2, TiO_2-SiO_2 and TiO_2-Al_2O_3, *Bull. Stand. J. Res.*, **11**, 725, (1933).

[24] Buscaglia, V., Nanni, P.: Decomposition of Al_2TiO_5 and $Al_{2(1-x)}Mg_xTi_{(1+x)}O_5$ ceramics, *J. Am. Ceram. Soc.*, **81**, [10], 2645 – 53, (1998).

[25] Venkataraman, R., Singh, P., Krishnamurthy, R.: Enhanced alpha phase stability during plasma spraying of alumina-13 mol% titania, J. *Am. Ceram. Soc.*, **89** [2], 734 – 736, (2006).

[26] Zaĭkin, A.E., Katulin, V.A., Levin, A.V., Petrov, A.L.: Hydrodynamic processes in a melt bath under laser-arc interaction conditions, Sov. J. Quantum Electron., **21**, [6], 635 – 639, (1991).

[27] Lu, Y., Chen, S.C.: Nanopatterning of a silicon surface by near-field enhanced laser irradiation, Nanotechnology, **14**, [4], 505 – 508, (2003).

[28] Alaverdyan, R.B., Grigoryan, A.M., Chilingaryan, Yu. S.: Convection in relatively thin layers of nematic liquid crystals, *J. Contemp. Phys. – Arme.*, **43**, [1], 19 – 22, (2008).